

Research Article

Adsorption Study for the Removal of Nitrate from Water Using Local Clay

A. Battas , A. El Gaidoumi, A. Ksakas, and A. Kherbeche

Laboratory of Catalysis, Materials and Environment, Higher School of Technology, Sidi Mohamed Ben Abdellah University, 30000 Fez, Morocco

Correspondence should be addressed to A. Battas; abdessamad.battas@usmba.ac.ma

Received 7 November 2018; Accepted 6 January 2019; Published 3 February 2019

Academic Editor: Cesar Mateo

Copyright © 2019 A. Battas et al. This is an open access article distributed under the Creative Commons Attribution License, which permits unrestricted use, distribution, and reproduction in any medium, provided the original work is properly cited.

Our research aimed at the removal of nitrate ions through adsorption by local clay. A series of batch experiments were conducted to examine the effects of contact time, adsorbent characteristics, initial concentration of nitrate, pH of the solution, concentration, and granulometry of adsorbent. Adsorption isotherms studies indicated that local clay satisfies Freundlich's model. The rate of reaction follows pseudo-second-order kinetics. Local clay successfully adsorbs nitrates at pH acid. The adsorption capacity under optimal conditions was found to be 5.1 mg/g. The adsorption yield increases with adsorbent dose and decrease with initial concentration of nitrate. The local clay was characterized by the X-ray fluorescence method (XRF), X-ray diffraction (XRD), Fourier transform-infrared spectroscopy (FTIR), scanning electronics microscopy (SEM), and measurement of specific surface area (BET). The results of the study indicated that local clay is useful materials for the removal of nitrates from aqueous solutions which can be used in water treatment without any chemical modification.

1. Introduction

Water resources are heavily polluted by several nitrogen compounds, such as nitrates, nitrites and ammonium. Agricultural, industrial and household wastewaters are the major sources of nitrates in the surface and ground waters [1]. Many investigations related the high nitrates concentration in water to the eutrophication in aquatic environment [2]. Excess nitrates in drinking water could potentially cause human health problems such as blue-baby syndrome in infants and stomach cancer in adults [3]. World Health Organization (WHO) recommended concentration limit in the drinking water as to not exceed 50 mg/L [4]. Therefore, numerous techniques for the removal of nitrates from water including adsorption, ion exchange, biological denitrification, chemical denitrification, electrodialysis and reverse osmosis, etc... [5]. Meanwhile, the adsorption is considered the most simple and efficient method [6, 7].

The application of local adsorbent for adsorption or elimination of nitrates present in wastewater is the object of the present study because of numerous economic advantages [8, 9]. In fact, clays are abundant and they present

excellent physicochemical stability and structural and surface properties [10]. Our investigations were focused on the following aspects: (1) adsorption behavior of nitrate using local clay, including isotherms studies and kinetics, in batch experiments; (2) the effect of contact time, adsorbent characteristics, initial concentration of nitrate, pH of solution, dose and granulometry of adsorbent on adsorption process.

2. Materials and Methods

2.1. Materials. The adsorption tests were carried out with greenish clay (A_1) rich in free silica (Quartz), found in large quantities in the northern region of Morocco. A synthetic solution of nitrate was prepared by dissolving 722 mg of potassium nitrate (KNO_3) in 1 L of distilled water. KNO_3 , chlorhydric acid (HCl), and Sodium hydroxide (NaOH) were purchased from Sigma-Aldrich.

2.2. Adsorbent Characterizations

2.2.1. X-Ray Fluorescence. The adsorbent chemical compositions were determined by the X-ray fluorescence, according

to the method given by Özcan et al. [11]. The energy spectrum allows the determination of the amount of elements based on their characteristic peaks. Thus, 1g of adsorbent was preliminary heated to 110°C for 24 hours to remove water contained in the sample and is then calcined at 1000°C for 5 min to transform it in its oxides, which will be evaluated by percentage weight. Analysis of the chemical compositions was achieved by Oxford MDX 1000.

2.2.2. X-Ray Diffraction (XRD). XRD analysis is based on constructive interference of monochromatic X-rays and a crystalline sample. Powder diffractograms were measured on an X'Pert PRO Analytical diffractometer ($\lambda_{\text{Cu-K}\alpha} = 1.54060\text{\AA}$) equipped with an X'Celerator scintillation detector operating at 30 mA and 40 kV from 10° to 80° with a scanning rate of 2° .min⁻¹.

2.2.3. Fourier Transform-Infrared Spectroscopy (FTIR). The vibrational behaviour of the respective samples was examined by Fourier transform infrared spectroscopy, in the range 400-4000 cm⁻¹ with resolution of 4 cm⁻¹, using FTIR spectrometer (Bruker Vertex 70). The samples were analysed in powder form (ATR technique).

2.2.4. Scanning Electronic Microscopy (SEM). The Scanning Electronic Microscopy is used to observe the texture of the clay sample and to characterize mineralogical assemblages. This analysis was carried out by Scanning Electronic Microscope, equipped with a probe EDAX, model QUANTA 200. The samples were analysed in pellet form.

2.2.5. Measurement of the Specific Surface Area. In this work the measurement of the specific surface of the adsorbent A₁ is very important to know the sites available for nitrate adsorption. The specific surface area was measured by the Brunauer-Emmett-Teller (BET) using AUTOSORB-1 system.

2.2.6. Laser Granulometric Analysis. The laser granulometric analysis (Beckman Coulter LS) of adsorbent A₁ has been determined by Fraunhofer method.

2.3. Dosage of Nitrate. In this work, we used the spectrometric method (UV-visible photolab 6600 spectrophotometer). In the presence of sodium salicylate, the nitrates give sodium parantrosalicylate, colored yellow and able to be determinate by spectrophotometer.

2.4. Adsorption Capacity. The choice of an adsorbent is based on its adsorption capacity expressed generally in mg pollutant/g adsorbent, itself related to the size of the specific surface and the total pore volume [12, 13]. To study the adsorption capacity of nitrate ions on the adsorbent A₁, 0.4 g of the adsorbent is introduced in 20 mL of a solution of nitrates (concentration of 100 mg/L), which corresponds to an initial charge of adsorbent of 20 g/L. Then, the mixture was stirred for 2 h on a magnetic stirrer (type SI Analytics GmbH) with the speed of 200 rpm at a temperature of 25°C

before to be filtered through at 0.45 μm filter membrane for analysis. The residual concentration of each sample allows determining the quantity of fixed nitrate ions per gram of adsorbent according to

$$q_t = \frac{(C_0 - C_t) * V}{m} \quad (1)$$

where, q_t is the amount of adsorbed ions per unit adsorbent at instant t (mg/g), m is the mass of adsorbent used (g), C_0 represents the initial concentration of nitrate ion in solution (mg/L), C_t is the concentration of nitrate ion in solution at instant t (mg/L) and V is the volume of solution used (L).

It is also possible to evaluate the quantity adsorbed by the adsorption yield given by

$$R (\%) = \frac{(C_0 - C_t)}{C_0} \quad (2)$$

where C_0 and C_t are the concentrations of nitrate at initial condition and at any time, respectively.

2.5. Adsorption Kinetics. The adsorption kinetics reflects the evolution of the adsorption process as a function of time, this is a key parameter considered when selecting an adsorbent [14]. Rapid adsorption is recommended for treatment methods using adsorption as a purification process [15]. Several models describing the diffusion of solutes at the surface and in the pores of the particles have been developed (film distribution model, intraparticulate diffusion model, diffusion model extra-particulate, pore diffusion model, etc.) [16]. However, in the case of nitrates, simplified models such as pseudo-first-order kinetics and pseudo-second-order kinetics were popular.

2.5.1. Pseudo First-Order Model. Lagergren showed that the adsorption rate of aqueous solution on the adsorbent is based on the adsorption capacity and following a first-order equation [17]. The nonlinear form of the first-order equation is given by

$$\frac{dq_t}{dt} = k_1 (q_e - q_t) \quad (3)$$

where q_t (mg.g⁻¹) is the adsorption capacity at time t , q_e (mg.g⁻¹) is the equilibrium adsorption capacity, and k_1 (min⁻¹) is the first-order constant.

After integration and application of the initial condition of $q = 0$ at $t = 0$, the equation takes the following form:

$$\log (q_e - q_t) = \log q_e - \frac{k_1 t}{2,303} \quad (4)$$

2.5.2. Pseudo Second-Order Model. The expression of the second-order was used to describe the kinetics of the adsorption processes. The pseudo second-order kinetic model equation is expressed as follows:

$$\frac{dq_t}{dt} = k_2 (q_e - q_t)^2 \quad (5)$$

where k_2 ($\text{g}\cdot\text{mg}^{-1}\text{ min}^{-1}$) is the rate constant of the pseudo second order.

The integration of this equation to $t = 0$ and $q_t = 0$ takes the linear form

$$\frac{t}{q_t} = \frac{1}{k_2 q_e^2} + \frac{t}{q_e} \quad (6)$$

2.6. Adsorption Isotherms. The adsorption isotherms are used to study the adsorption mechanisms. An adsorption isotherm describes the equilibrium at a given temperature between the adsorbed solute concentration and the unadsorbed concentration [18]. However, the literature shows that authors pay less attention to the type of isotherm obtained; they focus more on the mathematical model that translates the experimental results. Thus, two models are widely used: the Langmuir model (7) and the Freundlich model (8):

$$q_e = q_m \frac{b \cdot C_e}{1 + b \cdot C_e} \quad (7)$$

$$q_e = K_f \cdot C_e^{1/n} \quad (8)$$

where q_e (mg/g) is an adsorbed amount at equilibrium; C_e (mg/L) is a concentration at equilibrium; q_m (mg/g) is a maximum adsorption capacity of the monolayer; K_f and n are the parameters of Freundlich; b is the parameter of Langmuir.

The Langmuir model assumes that (1) the adsorption is monolayer, (2) it is reversible, (3) each site can adsorb only one ion, and (4) there is no interaction between the ions with adsorbent. The Freundlich model suggests that binding energy decreases exponentially with increasing surface saturation. This model is widely used, although it is empirical. It gives an indication of surface heterogeneity [19].

2.6.1. Freundlich Isotherm. The linear form of the equation of Freundlich can be written in logarithmic form according to the following relation:

$$\log q_e = \log K_f + \frac{1}{n} \log C_e \quad (9)$$

where K_f and $1/n$ are the constants of Freundlich connected to the adsorption capacity and the intensity of adsorption of the adsorbent, respectively.

2.6.2. Langmuir Isotherm. By applying the Langmuir hypothesis, it can be concluded that in the case of a large quantity of adsorbed solute, the parameter $b \cdot C_e$ becomes considerably greater than 1. This implies that q tends to q_m [20]. The linear form of the Langmuir equation is

$$\frac{C_e}{q} = \frac{1}{q_m \cdot b} + \frac{C_e}{q_m} \quad (10)$$

2.7. Study of the Parameters Effect

2.7.1. Adsorption Tests. The adsorption tests were carried out in batch mode in beakers containing 20 mL of the solution to be treated, mounted on a thermoregulated agitating platform.

A solution of KNO_3 was used as a source of nitrate ions under the following working conditions: the initial concentration of NO_3^- varies from 50 to 200 mg/L, the adsorbent dose varies from 5 to 40 g/L, and the pH is from 2 to 9, with a contact time set at 120 min and a stirring speed of 200 rpm at constant temperature of 25°C. Finally, the solutions were filtered and the filtrate was recovered for analysis.

2.7.2. The Adsorbent Dose Effect. The effect of the adsorbent filler on the retention of nitrate ions was studied for the values of 5, 10, 20, and 40 g/L of adsorbent A_1 while keeping the other parameters fixed (room temperature, agitation speed of 200 rpm, and the initial nitrate concentration is 100 mg/L).

2.7.3. The Initial Concentration Effect. In order to study the effect of the initial concentration on the adsorption of nitrate ions, variable NO_3^- concentrations (50, 100, 150, and 200 mg/L) with an adsorbent load of 20 g/L of adsorbent A_1 were used.

2.7.4. The pH Effect. The pH is an important parameter to be considered in sorption processes because it may affect both the properties of the adsorbent and the composition of the solution [21]. The study of the pH effect on the adsorption of nitrate ions was carried out by varying the pH from 2 to 9 with an initial concentration of NO_3^- ions (100 mg/L) and adsorbent dose fixed at 20 g/L at room temperature. The initial pH of the solutions was measured by a pH-meter and adjusted to the desired values using 0.01N HCl and NaOH solutions.

2.7.5. Adsorbent Granulometry Effect. The effect of the granulometry was studied by the use of adsorbent with particle sizes: $d < 110 \mu\text{m}$, $200 \mu\text{m} < d < 400 \mu\text{m}$, and $d > 400 \mu\text{m}$.

3. Results and Discussion

3.1. Characterization of Adsorbent

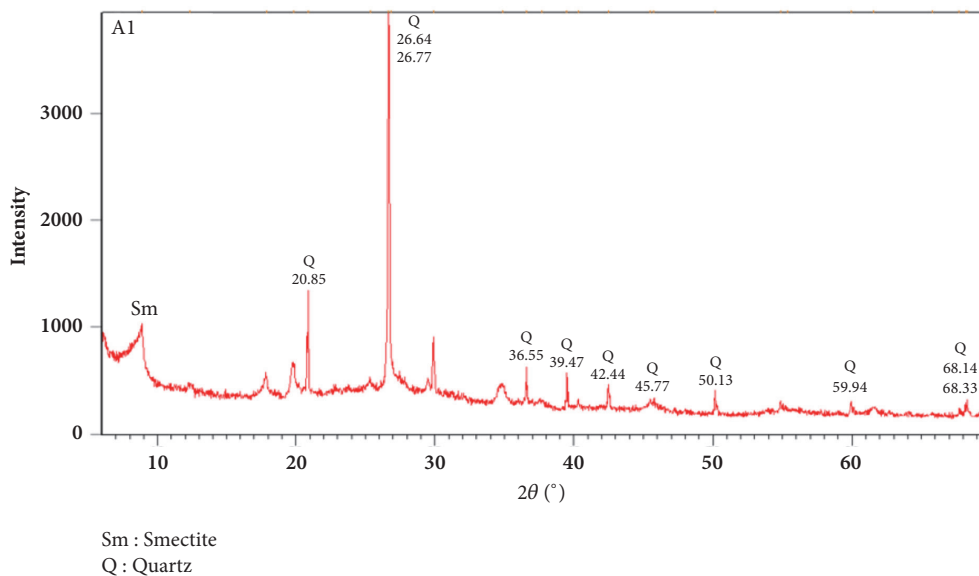
3.1.1. Chemical Compositions of Adsorbent by X-Ray Fluorescence. To determine the chemical compositions of studied adsorbent, we conducted a spectrometry analyses XRF. Table 1 shows the material analyses results by X-ray fluorescence spectrometry.

The analyses carried out on the investigated adsorbent (Table 1) show that the mass ratio $\text{SiO}_2/\text{Al}_2\text{O}_3$ is 4.24. This high value suggests the presence of a large amount of free silica (Quartz). A_1 showed 7.80 % of loss-on-ignition (LOI) may be due to the dehydroxylation of the clay and removal of its organic and carbonate compounds.

3.1.2. X-Ray Diffraction Analysis. A mineralogical analysis of the raw sample of adsorbent A_1 was achieved by X-ray diffraction in order to identify the main adsorbent minerals. The diffractogram of the adsorbent sample A_1 (Figure 1) showed that this material is mostly composed of quartz with peaks located at 2θ -angles ($^\circ$): 20.85, 26.77, 36.55, 39.47, 42.44, 45.77, 50.13, 59.94, and 68.33.

TABLE 1: Chemical compositions of the adsorbent A₁ in (%).

Components	SiO ₂	Al ₂ O ₃	Fe ₂ O ₃	CaO	MgO	SO ₃	K ₂ O ₃	Na ₂ O	LOI
Wt. (%)	63.00	14.85	5.02	1.11	2.65	0.06	5.14	0.06	7.80

FIGURE 1: XRD spectrum of adsorbent A₁.

3.1.3. Fourier Transforms Infrared Spectroscopy Analysis. The FTIR spectroscopy analysis gets absorption bands corresponding to the various vibrations of the characteristic bonds of the phases already detected by XRD. The FTIR spectrum of adsorbent A₁ (Figure 2) showed several absorption bands the peak to 3606 cm^{-1} assigned to the vibration band of the hydroxyl group. Broad bands located at 3397 and 1636 cm^{-1} are the cause of the axial and angular deformation of water molecules adsorbed between sheets [22]. The centred strips at 797 and 1442 cm^{-1} correspond to the stretching of the vibrations of Si-O in SiO₂ and CO₃, respectively, while the band at 508 cm^{-1} is probably assigned to the vibrations of the connections Si-O-Si of quartz. Vibration bands located at 692 and 909 cm^{-1} are assigned to deformation of Si-O-Al and Al-OH, respectively. Table 2 represents the vibration bands and their assignments for adsorbent A₁.

3.1.4. Measurement of the Specific Surface Area. The specific surface area and total pore volume of the adsorbent A₁ were determined as $38.08\text{ m}^2\text{ g}^{-1}$ and $8.75\text{ cm}^3\text{ g}^{-1}$, respectively, a bit larger than that of purified montmorillonite ($34\text{ m}^2\text{ g}^{-1}$) of commercial Argentine bentonite [23]. We displayed in Table 3 features of the present adsorbent compared to those of some other adsorbents reported in the literature.

3.1.5. Laser Granulometric Analysis. The particle size, shape and distribution have been reported to be a very important property in determining the industrial uses of clays [27]. For this purpose, Beckman Coulter LS Particle Size Analyzer was used to determine the granulometric parameters d_{10} , d_{50} ,

and d_{90} of the local clay A₁. The cumulative and differential particle size distributions of this material are presented in Figure 3 resulting in 2.10 , 25.47 , and $110.10\text{ }\mu\text{m}$, for d_{10} , d_{50} , and d_{90} , respectively. The effect of the adsorbent granulometry on the adsorption of nitrate will be presented in Section 3.4.4.

3.1.6. Scanning Electron Microscopy (SEM). The images obtained by scanning electron microscopy of the adsorbent sample with three different magnifications are shown in Figure 4. The image of the local clay A₁ indicates that the adsorbent particles are in the form of platelets in the pace of leaves with irregular contours [28, 29]. This is a morphology encountered both for Kaolinites poorly crystallized only for Illites as observed by Konan et al. [30].

3.2. Adsorption Kinetics

3.2.1. Contact Time. The capacity adsorption of nitrate ions solution 100 mg/L on an adsorbent dose 20 g/L was followed as a function of time (h). The results presented in Figure 5 show that the adsorption capacity of the nitrate ions increases with contact time and reaches a maximum value at 2 h. After 2 h, the adsorption capacity decreases. This decrease can be explained by the saturation of the free adsorbent sites and may be due to an adsorbate release. According to the Freundlich hypothesis, the binding energy decreases exponentially with increasing surface saturation [31].

3.2.2. Pseudo First-Order Model. The reaction order is determined by the following operating conditions: the nitrate

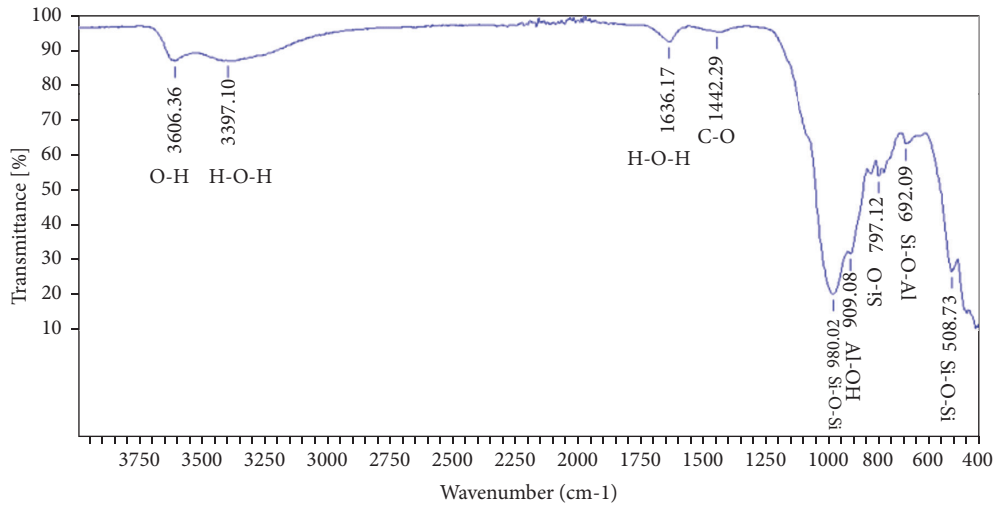


FIGURE 2: FTIR spectrum to Fourier transforms of adsorbent A₁.

TABLE 2: Infrared analysis results of different vibration bands.

Adsorbent	Vibration bands (cm ⁻¹)	Assignment
Adsorbent A ₁	3606	Vibration of the hydroxyl group
	3397-1636	Axial and angular deformation of water molecules
	1442	Vibration stretch of CO ₃
	909	Deformation of Al-OH
	797	Vibration stretch of Si-O
	692	Deformation of Si-O-Al
	508	Vibration of links Si-O-Si

TABLE 3: Comparison of BET surface area of local adsorbent studied A₁ with other adsorbents.

The sample	Specific surface in m ² .g ⁻¹	References
Montmorillonite	34	[23]
Smectite	31.13	[24]
Illite	25	[25]
Kaolinite	21	[26]
Adsorbent A ₁	38.08	Present study

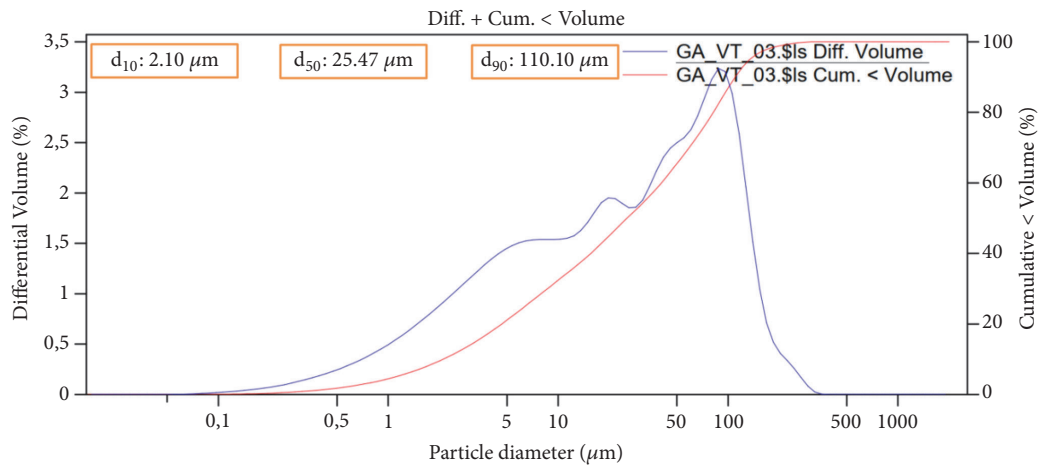


FIGURE 3: Granulometric distribution of adsorbent A₁.

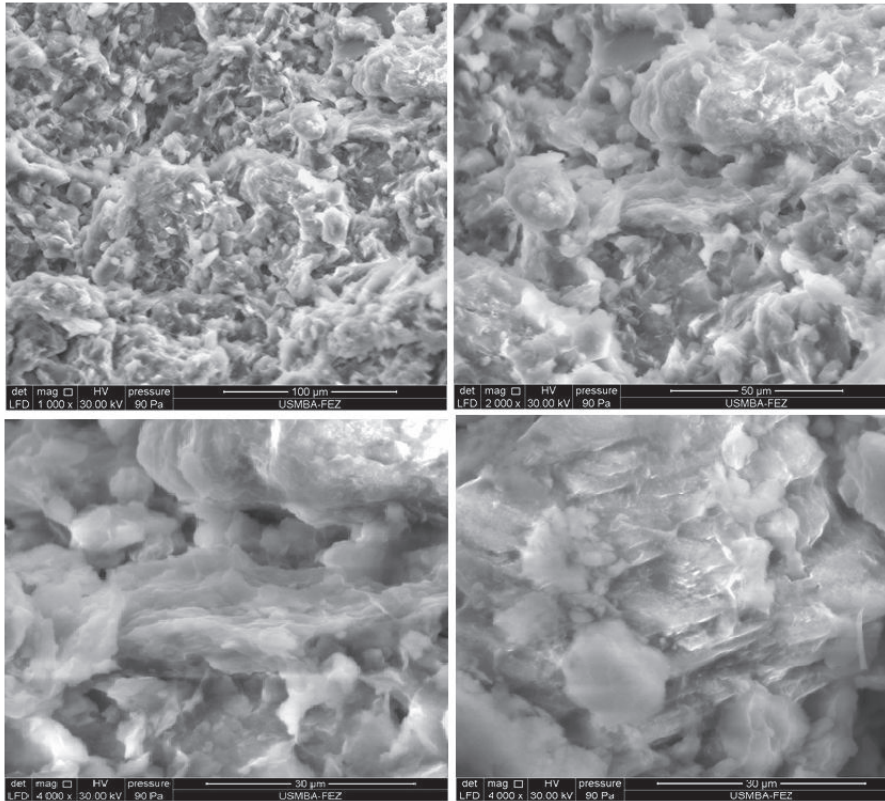


FIGURE 4: SEM images of adsorbent A₁ with three different resolutions 100, 50 and 30 μm .

TABLE 4: Kinetic parameters of pseudo-first order and pseudo-second-order models.

Adsorbent	Pseudo first order			Pseudo second order		
	k_1 (h^{-1})	q_e (mg/g)	R^2	k_2 (g/mg.h)	q_e (mg/g)	R^2
Adsorbent A ₁	2.014	0.516	0.937	10.542	0.384	0.952

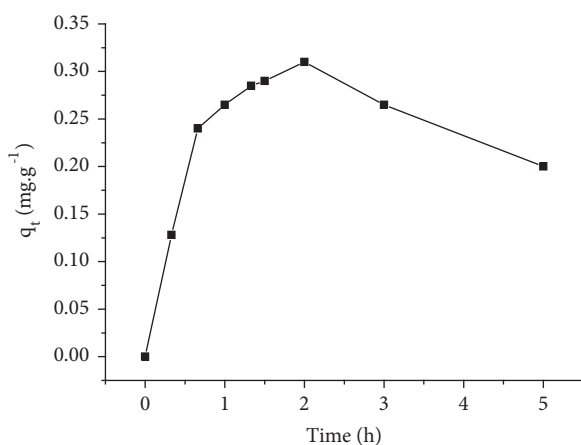


FIGURE 5: Evolution of the adsorption capacity of nitrates on adsorbent A₁.

concentration solution of 100 mg/L, the adsorption dose of 20 g/L, the temperature of 25°C, and the stirring speed of 200

rpm. Figure 6 represents the adsorption kinetics of the nitrate ions on the adsorbent A₁ according to the pseudo-first-order kinetic model. The linear equation is presented by (4).

3.2.3. Pseudo Second-Order Model. The Figure 7 shows the adsorption kinetics of the nitrate ions on the adsorbent A₁ according to the pseudo-second-order kinetic model. The linear equation is presented by (6). Table 4 indicates that the adsorption kinetics of nitrate ions onto the adsorbent A₁ is better described by the pseudo second-order model. The correlation coefficient is close to unity ($R^2 = 0.952$), and the value of q_e calculated by the pseudo second-order model is very similar to that determined experimentally.

3.3. Adsorption Isotherms. The adsorption isotherms of nitrate ions onto the adsorbent A₁ is studied by the representation of the equilibrium adsorption capacity variation q_e (mg/g) as a function of the equilibrium concentration of nitrate (mg/L), according to the Freundlich and Langmuir models, represented by Figures 8 and 9 respectively. The obtained results are grouped in Table 5.

TABLE 5: Parameters of isotherm models for the nitrate ions adsorption onto the adsorbent A₁.

Adsorbent	Freundlich model			Langmuir model		
	K _f	n _f	R ²	b	q _m (mg/g)	R ²
A ₁	0.145	1.176	0.990	3.54*10 ⁻³	27.77	0.8327

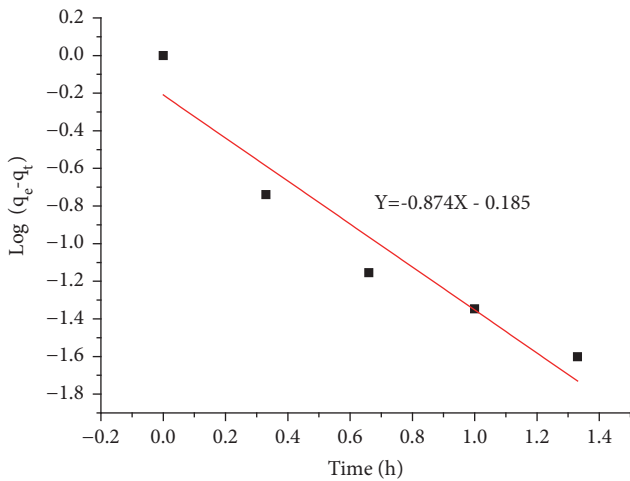


FIGURE 6: The adsorption kinetics of the nitrate ions on the adsorbent A₁ according to the pseudo-first-order kinetic model.

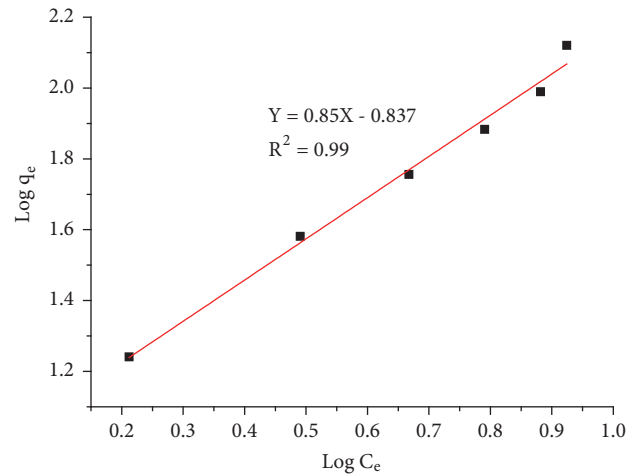


FIGURE 8: Adsorption Isotherm of the nitrate ions onto the adsorbent A₁ according to the Freundlich model.

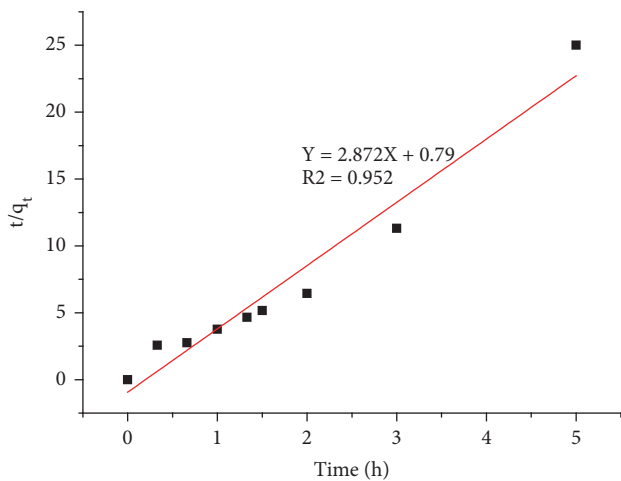


FIGURE 7: The adsorption kinetics of the nitrate ions on the adsorbent A₁ according to the pseudo second-order kinetic model.

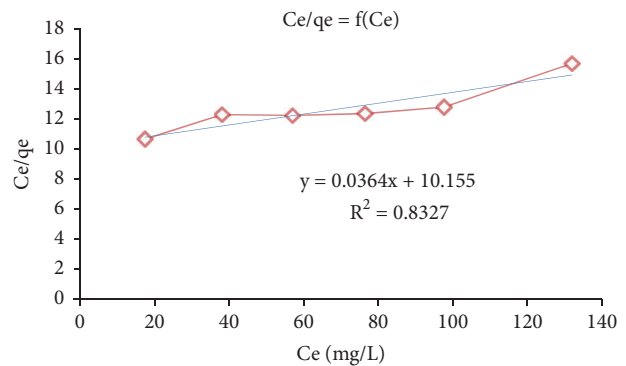


FIGURE 9: Adsorption isotherm of the nitrate ions onto the adsorbent A₁ according to the Langmuir model.

From the results shown in Table 5, it can be said that the adsorption of nitrate ions on the adsorbent A₁ is best described by the Freundlich model (correlation factor close to the unit R² = 0.99). According to Freundlich hypotheses, the adsorption energy of nitrate ions on the adsorbent A₁ decreases exponentially with increasing surface saturation and the surface of the adsorbent is heterogeneous [32, 33].

3.4. Parameters Effects on Adsorption of Nitrate Ions

3.4.1. *Effect of Adsorbent Dose.* The adsorbent dose effect was investigated at room temperature for an initial concentration of NO₃⁻ (100 mg/L) with stirring at 200 rpm for 120 min. The variation influence of the adsorbent dose is shown in Figure 10.

Figure 10 shows that the adsorption efficiency increases with increasing the adsorbent dose. This can be explained by the increase in the number of active adsorption sites, and the availability of the adsorption sites increases the adsorption capacity. The adsorption yields vary from 16 to 35% and better adsorption efficiency of 35% is observed for a concentration of adsorbent A₁ at 40 g/L.

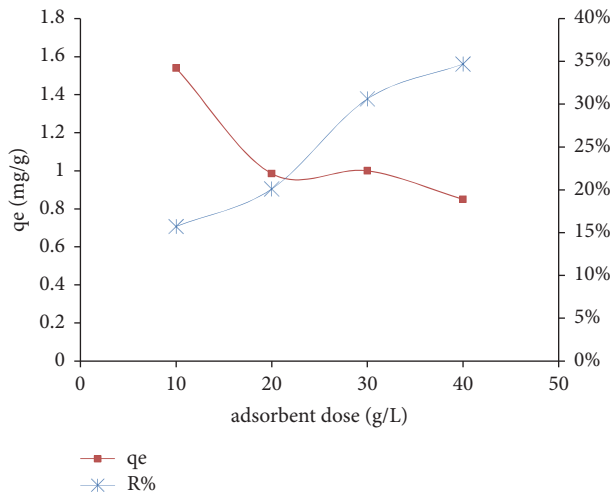


FIGURE 10: Effect of the adsorbent dose (adsorbent A_1) on the adsorption of nitrate ions.

Figure 10 also shows the adsorption capacity (mg/g) of NO_3^- depending on the adsorbent support in the solution. The curve follows a downward trend, indicating that the amounts of NO_3^- adsorbed by the adsorbent A_1 are inversely proportional to the adsorbent dose. Indeed, it is noted that q_e reaches a maximum of 1.54 mg/g for an adsorbent concentration equal to 10 g/L, while the lowest q_e is 0.7 mg/g, for an adsorbent concentration of 40 g/L.

3.4.2. Initial Nitrate Concentration Effect. The initial nitrate concentration effect was investigated at NO_3^- concentrations (50, 100, 150, and 200 mg/L), and the adsorption tests were carried out at room temperature with stirring at 200 rpm for 120 min with 20 g/L of adsorbent A_1 . Figure 11 shows the results of the yield and adsorption capacity as a function of the initial concentration of the nitrate ions.

The adsorption efficiency evolution as a function of the initial concentration of NO_3^- follows a decreasing curve and thus the highest yields are observed for the lowest initial NO_3^- concentrations. Indeed, the highest adsorption yield of nitrate ions (32%) is observed for an initial concentration of NO_3^- in the solution equal to 50 mg/L. This yield decreases from 32% to 14% by varying the initial concentration of nitrate ions from 50 to 200 mg/L. That is, the adsorption capacity increases from 0.8 mg/g to 1.35 mg/g.

3.4.3. pH Effect. The pH effect on the adsorption of nitrate ions was investigated by carrying out adsorption tests over a pH range from 2 to 9. The results are shown in Figure 12.

The pH of the solution is a very important parameter in the study of the adsorption of nitrate ions by clay. Figure 12 shows the variation of the adsorption capacity of NO_3^- depending on the pH of a solution containing 100 mg/L of NO_3^- and 20 g/L of the A_1 adsorbent. It is observed that the adsorption capacity q_e reaches their maximum at pH 2 and decrease with the increase in pH. Usually, the influence of pH on anion exchange reaction was mainly due to the

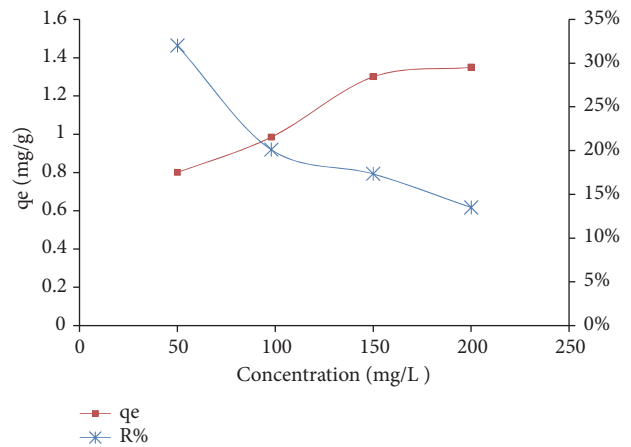


FIGURE 11: Effect of the initial concentration of NO_3^- .

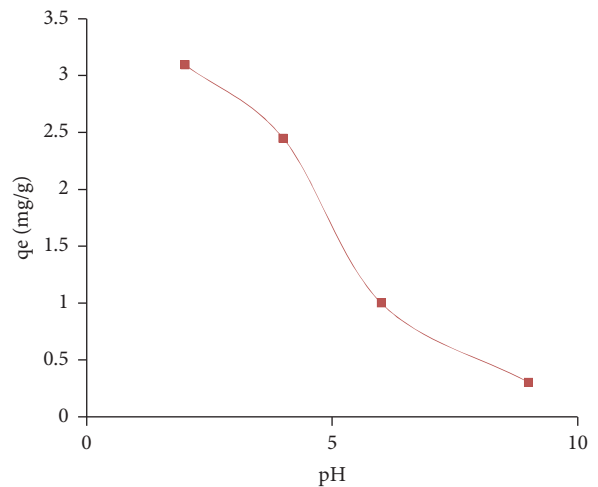


FIGURE 12: pH effect on the adsorption of NO_3^- .

competition between the hydroxyl ions and anions. When pH of the solution increases, the surface becomes negatively charged and the adsorption capacity for nitrate decreases, because negatively charged surface sites on the adsorbent did not favor nitrate due to the electrostatic repulsion [34, 35].

3.4.4. Adsorbent Granulometry Effect. The effect of the particle size distribution on the adsorption of nitrate is represented by Figure 13. The results show that the particle size of the adsorbent A_1 influences the adsorption capacity of the nitrate ions. The adsorption capacity reaches a maximum value for a granulometry of the adsorbent of $d < 110 \mu\text{m}$. This can be explained by the increase of the specific adsorption sites [36].

4. Conclusions

This study investigated the adsorption characteristics of local clay A_1 as a potential adsorbent for the removal of nitrate from aqueous solutions using batch system. The experimental parameters were very important in order to understand the mechanism of adsorption of nitrate ions, such

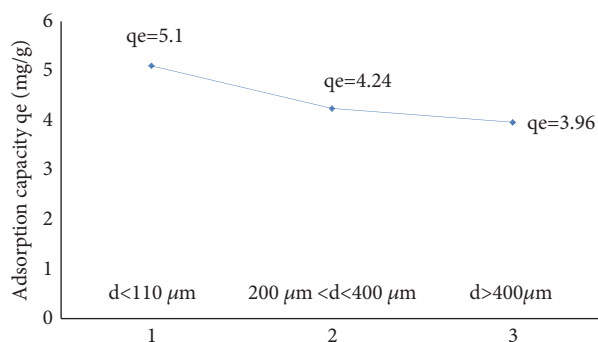


FIGURE 13: Effect of particle size on the adsorption of NO_3^- ions onto A_1 .

as the initial nitrate ion concentration, adsorbent dose, pH, and particle size. The results showed that the adsorption efficiency increased with the adsorbent dose and decreases with the initial concentration. The pH optimum for nitrate ions adsorption onto the adsorbent A_1 is between 2 and 4. The adsorption capacity reaches a maximum value for the adsorbent granulometry from $d < 110 \mu\text{m}$. Adsorption equilibrium applied by Langmuir and Freundlich allowed us to conclude that Freundlich's model shows the best correlation. The adsorption kinetics of nitrate ions on the adsorbent A_1 is better described by the pseudo second-order model. The choice of this clay presents the opportunity to benefit from this cheap material found in nature with significant quantities.

Data Availability

The data used to support the findings of this study are available from the corresponding author upon request.

Conflicts of Interest

The authors declare that they have no conflicts of interest.

Acknowledgments

The authors thank Professor Brahim El Bali, associate member of our Laboratory, for his collaboration in interpretations of characterization techniques (FTIR, XRD, and BET).

References

- [1] Y. Wu, Y. Wang, J. Wang et al., "Nitrate removal from water by new polymeric adsorbent modified with amino and quaternary ammonium groups: Batch and column adsorption study," *Journal of the Taiwan Institute of Chemical Engineers*, vol. 66, pp. 191–199, 2016.
- [2] S. P. Boeykens, M. N. Piol, L. S. Legal, A. B. Saralegui, and C. Vázquez, "Eutrophication decrease : phosphate adsorption process in presence of nitrates," *Journal of Environmental Management*, vol. 203, pp. 888–895, 2017.
- [3] M. H. Ward and J. D. Brender, "Drinking water Nitrate and Human Health," *Encyclopedia of Environmental Health*, pp. 167–178, 2011.
- [4] World Health Organization, *Revisions of the WHO Guidelines for Drinking Water Quality Report on a WHO Consultation*, WHO Regional Office for Europe, Medmenham, UK, 1992.
- [5] M. Daud, Z. Khan, A. Ashgar, M. I. Danish, and I. A. Qazi, "Comparing and optimizing nitrate adsorption from aqueous solution using Fe/Pt bimetallic nanoparticles and anion exchange resins," *Journal of Nanotechnology*, vol. 2015, Article ID 985984, 7 pages, 2015.
- [6] R. Srinivasan, "Advances in application of local adsorbent and its composites in removal of biological, organic, and inorganic contaminants from drinking water," *Advances in Adsorbent Science and Engineering*, vol. 2011, Article ID 872531, 17 pages, 2011.
- [7] A. Bhatnagar, M. Ji, Y.-H. Choi et al., "Removal of nitrate from water by adsorption onto zinc chloride treated activated carbon," *Separation Science and Technology*, vol. 43, no. 4, pp. 886–907, 2008.
- [8] M. F. Abou Taleb, G. A. Mahmoud, S. M. Elsigeny, and E.-S. A. Hegazy, "Adsorption and desorption of phosphate and nitrate ions using quaternary (polypropylene-g-N,N-dimethylamino ethylmethacrylate) graft copolymer," *Journal of Hazardous Materials*, vol. 159, no. 2-3, pp. 372–379, 2008.
- [9] A. Bhatnagar and M. Sillanpää, "A review of emerging adsorbents for nitrate removal from water," *Chemical Engineering Journal*, vol. 168, no. 2, pp. 493–504, 2011.
- [10] A. U. Baes, T. Okuda, W. Nishijima, E. Shoto, and M. Okada, "Adsorption and ion exchange of some groundwater anion contaminants in an amine modified coconut coir," *Water Science and Technology*, vol. 35, no. 7, pp. 89–95, 1997.
- [11] A. Özcan, M. Şahin, and A. S. Özcan, "Adsorption of Nitrate Ions onto Sepiolite and Surfactant-Modified Sepiolite," *Adsorption Science & Technology*, vol. 23, no. 4, pp. 323–334, 2005.
- [12] D. Z. Borislav, J. C. Jiří, S. Martin, and J. Josef, "Pore classification in the characterization of porous materials: a perspective," *Central European Journal of Chemistry*, vol. 5, no. 4, pp. 385–395, 2007.
- [13] B. He and W. Huang, *Ion Exchange and Adsorption Resin*, Shanghai Scientific and Technology Education Publishing, Shanghai, China, 2nd edition, 1995.
- [14] C. Fan and Y. Zhang, "Adsorption isotherms, kinetics and thermodynamics of nitrate and phosphate in binary systems on a novel adsorbent derived from corn stalks," *Journal of Geochemical Exploration*, vol. 188, pp. 95–100, 2018.
- [15] S. Vasudevan, "Process conditions and kinetics for the removal of copper from water by electrocoagulation," *The Canadian Journal of Chemical Engineering*, vol. 90, pp. 1017–1026, 2012.
- [16] C. Tien and B. V. Ramarao, "Further examination of the relationship between the Langmuir kinetics and the Lagergren and the second-order rate models of batch adsorption," *Separation and Purification Technology*, vol. 136, pp. 303–308, 2014.
- [17] R.-L. Tseng, F.-C. Wu, and R.-S. Juang, "Characteristics and applications of the Lagergren's first-order equation for adsorption kinetics," *Journal of the Taiwan Institute of Chemical Engineers*, vol. 41, no. 6, pp. 661–669, 2010.
- [18] S. Chatterjee and S. H. Woo, "The removal of nitrate from aqueous solutions by chitosan hydrogel beads," *Journal of Hazardous Materials*, vol. 164, no. 2-3, pp. 1012–1018, 2009.

- [19] D. Myers, *Surfaces, Interfaces, and Colloids: Principles and Applications*, John Wiley & Sons Inc., New York, NY, USA, 2nd edition, 1999.
- [20] A. Dağbrowski, "Adsorption—from theory to practice," *Advances in Colloid and Interface Science*, vol. 93, no. 1–3, pp. 135–224, 2001.
- [21] R. Alfaro-Cuevas-Villanueva, A. Roxana Hidalgo-Vázquez, C. J. C. Penagos, and R. Cortés-Martínez, "Thermodynamic, kinetic, and equilibrium parameters for the removal of lead and cadmium from aqueous solutions with calcium alginate beads," *The Scientific World Journal*, vol. 2014, Article ID 647512, 10 pages, 2014.
- [22] R. I. Iliescu, E. Andronescu, C. D. Ghitulica, G. Voicu, A. Ficai, and M. Hoteteu, "Montmorillonite-alginate nanocomposite as a drug delivery system - Incorporation and in vitro release of irinotecan," *International Journal of Pharmaceutics*, vol. 463, no. 2, pp. 184–192, 2014.
- [23] A. P. Magnoli, L. Tallone, C. A. R. Rosa, A. M. Dalcero, S. M. Chiacchiera, and R. M. T. Sanchez, "Commercial bentonites as detoxifier of broiler feed contaminated with aflatoxin," *Applied Clay Science*, vol. 40, no. 1–4, pp. 63–71, 2008.
- [24] U. Kuila, D. K. McCarty, A. Derkowski, T. B. Fischer, T. Topór, and M. Prasad, "Nano-scale texture and porosity of organic matter and clay minerals in organic-rich mudrocks," *Fuel*, vol. 135, pp. 359–373, 2014.
- [25] H. V. Olphen and J. J. Fripiat, *Data Handbook for Adsorbent Minerals and Other Nonmetallic Minerals*, Pergamon Press, Oxford, UK, 1979.
- [26] C. T. Chiou, D. W. Rutherford, and M. Manes, "Sorption of nitrogen and ethylene glycol monoethyl ether (EGME) vapors on some soils, clays, and mineral oxides and determination of sample surface areas by use of sorption data," *Environmental Science & Technology*, vol. 27, no. 8, pp. 1587–1594, 1993.
- [27] H. H. Murray, "Traditional and new applications for kaolin, smectite, and palygorskite: a general overview," *Applied Clay Science*, vol. 17, no. 5–6, pp. 207–221, 2000.
- [28] B. Zsirka, E. Horváth, Z. Járvas, A. Dallos, É. Makó, and J. Kristóf, "Structural and energetical characterization of exfoliated kaolinite surfaces," *Applied Clay Science*, vol. 124–125, pp. 54–61, 2016.
- [29] Z. Sun, G. Yao, X. Zhang, S. Zheng, and R. L. Frost, "Enhanced visible-light photocatalytic activity of kaolinite/g-C₃N₄ composite synthesized via mechanochemical treatment," *Applied Clay Science*, vol. 129, pp. 7–14, 2016.
- [30] K. L. Konan, C. Peyratout, A. Smith, J.-P. Bonnet, P. Magnoux, and P. Ayrault, "Surface modifications of illite in concentrated lime solutions investigated by pyridine adsorption," *Journal of Colloid and Interface Science*, vol. 382, no. 1, pp. 17–21, 2012.
- [31] N. Dammak, N. Fakhfakh, S. Fourmentin, and M. Benzina, "Treatment of gas containing hydrophobic VOCs by adsorption process on raw and intercalated clays," *Research on Chemical Intermediates*, vol. 41, no. 8, pp. 5475–5493, 2015.
- [32] E. Bulut, M. Özacar, and I. A. Şengil, "Adsorption of malachite green onto bentonite: equilibrium and kinetic studies and process design," *Microporous and Mesoporous Materials*, vol. 115, no. 3, pp. 234–246, 2008.
- [33] A. Q. Selim, E. A. Mohamed, M. Mobarak, A. M. Zayed, M. K. Seliem, and S. Komarneni, "Cr(VI) uptake by a composite of processed diatomite with MCM-41: Isotherm, kinetic and thermodynamic studies," *Microporous and Mesoporous Materials*, vol. 260, pp. 84–92, 2018.
- [34] L. A. Richards, M. Vuachère, and A. I. Schäfer, "Impact of pH on the removal of fluoride, nitrate and boron by nanofiltration/reverse osmosis," *Desalination*, vol. 261, no. 3, pp. 331–337, 2010.
- [35] Y. Cengeloglu, A. Tor, M. Ersoz, and G. Arslan, "Removal of nitrate from aqueous solution by using red mud," *Separation and Purification Technology*, vol. 51, no. 3, pp. 374–378, 2006.
- [36] C. H. Giles, T. H. McEwan, S. N. Nakhwa, and D. Smith, "Studies in adsorption. Part XI. A system of classification of solution adsorption isotherms, and its use in diagnosis of adsorption mechanisms and in measurement of specific surface areas of solids," *Journal of the Chemical Society*, vol. 3, pp. 3973–3993, 1960.